

Metastable phase transformation and hcp- ω transformation pathways in Ti and Zr under high hydrostatic pressures

Lei Gao, Xiangdong Ding, Turab Lookman, Jun Sun, and E. K. H. Salje

Citation: [Applied Physics Letters](#) **109**, 031912 (2016); doi: 10.1063/1.4959864

View online: <http://dx.doi.org/10.1063/1.4959864>

View Table of Contents: <http://scitation.aip.org/content/aip/journal/apl/109/3?ver=pdfcov>

Published by the [AIP Publishing](#)

Articles you may be interested in

[Phase stability limit of c-BN under hydrostatic and non-hydrostatic pressure conditions](#)

J. Chem. Phys. **140**, 164704 (2014); 10.1063/1.4871897

[Phase transformations and vibrational properties of coronene under pressure](#)

J. Chem. Phys. **139**, 144308 (2013); 10.1063/1.4824384

[High-temperature phase transitions in Cs H₂ P O₄ under ambient and high-pressure conditions: A synchrotron x-ray diffraction study](#)

J. Chem. Phys. **127**, 194701 (2007); 10.1063/1.2804774

[Analysis of the equations-of-state of water in the metastable region at high pressures](#)

J. Chem. Phys. **116**, 8632 (2002); 10.1063/1.1471554

[Relaxation and phase transformations in simple atomic systems with short range interactions](#)

AIP Conf. Proc. **513**, 90 (2000); 10.1063/1.1303335

The image shows the cover of an Applied Physics Reviews journal. It features a blue background with a molecular structure of spheres and sticks. On the left, there is a small inset image of the journal cover, which shows a diagram of a device structure. The main text on the right reads 'NEW Special Topic Sections' in large white letters. Below this, it says 'NOW ONLINE' in yellow, followed by 'Lithium Niobate Properties and Applications: Reviews of Emerging Trends' in white. The AIP Applied Physics Reviews logo is in the bottom right corner.

NEW Special Topic Sections

NOW ONLINE
Lithium Niobate Properties and Applications:
Reviews of Emerging Trends

AIP Applied Physics
Reviews

Metastable phase transformation and hcp- ω transformation pathways in Ti and Zr under high hydrostatic pressures

Lei Gao,^{1,a)} Xiangdong Ding,^{1,b)} Turab Lookman,² Jun Sun,¹ and E. K. H. Salje^{1,3,b)}

¹State Key Laboratory for Mechanical Behavior of Materials, Xi'an Jiaotong University, Xi'an 710049, China

²Theoretical Division, Los Alamos National Laboratory, Los Alamos, New Mexico 87545, USA

³Department of Earth Sciences, University of Cambridge, Cambridge CB2 3EQ, United Kingdom

(Received 1 June 2016; accepted 13 July 2016; published online 22 July 2016)

The energy landscape of Zr at high hydrostatic pressure suggests that its transformation behavior is strongly pressure dependent. This is in contrast to the known transition mechanism in Ti, which is essentially independent of hydrostatic pressure. Generalized solid-state nudged elastic band calculations at constant pressure shows that α -Zr transforms like Ti only at the lowest pressure inside the stability field of ω -phase. Different pathways apply at higher pressures where the energy landscape contains several high barriers so that metastable states are expected, including the appearance of a transient bcc phase at ca. 23 GPa. The global driving force for the hcp- ω transition increases strongly with increasing pressure and reaches 23.7 meV/atom at 23 GPa. Much of this energy relates to the excess volume of the hcp phase compared with its ω phase. © 2016 Author(s). All article content, except where otherwise noted, is licensed under a Creative Commons Attribution (CC BY) license (<http://creativecommons.org/licenses/by/4.0/>). [<http://dx.doi.org/10.1063/1.4959864>]

Group IV transition metals Ti and Zr play a major role in aerospace and nuclear industries. They have large strength-to-weight ratios, excellent corrosion and oxidation resistance and low neutron-capture cross-section.^{1–7} Their applicability is limited by the hcp (α)-simple hexagonal (ω) phase transformation under high hydrostatic pressure.^{4–9} The appearance of the ω phase can strengthen the metal,^{10,11} while it also greatly lowers its toughness and ductility.^{7–9} Extensive research has been undertaken to identify, and possibly modify, the mechanism of the hcp- ω phase transformation.^{4,7,8,12–23}

From a more fundamental perspective, the α - ω phase transition is a prototype for high pressure structural transformation processes in simple crystal structures, their kinetics, and the influence of impurities on the phase boundary among other aspects of the phase relationship. The transition mechanism in Zr is considered as a model for the transitions in Pu, which is much harder to investigate. Such transformations are also very common in the geological context where many minerals show high pressure transformations with complex transformation pathways.^{24–26} One key observation from such studies is that pressure transformations may not occur instantaneously but follow time dependent transition mechanisms, which may involve metastable intermediate structural states. Such behavior was indeed found in the studies of the kinetics of the α - ω phase transition in zirconium.^{9,27} These authors observed a clear time and pressure dependence of the transition as function of driving pressure and used the data to fit kinetics models, which gave some insight into transformation mechanism that influences the transformation kinetics. These studies are fundamentally important because it questions the simple equilibrium transformation behavior via heterogeneous transformations and opens the way to

investigate scenarios where Zr can first be subjected to high pressure and then transforms at this pressure kinetically. This means that Zr may form interesting metastable states and, as we will argue, may indeed form metastable bcc Zr (equivalent to the high temperature β phase). We will show in this paper that the metastable bcc phase will occur only at very high pressures so that the experimental conditions in the Jacobsen study²⁷ were unable to observe this state. We mention that fast kinetics can play a role in nuclear processes, where swift heavy metal irradiation can indeed generate metastable states.²⁸ Some related experimental evidence for an intermediate bcc state in Ti-V alloys was also reported by Vohra *et al.*²⁹

The expected “equilibrium” transition in Zr is well researched. Initial work in this area focused on orientation relationships between initial phase and final product,⁹ followed by some initial kinetics.^{18–21} Several transformation pathways were suggested: Silcock’s supposed two orientation relationships that would define the transition.¹³ This idea was partially supported by Wenk *et al.*⁴ from diffraction experiments. It was also speculated that the ω phase was the result of quenching the high temperature bcc phase⁹ while Jyoti *et al.*²¹ suggested that the bcc phase appears as an unstable intermediary between the two and established a correspondence matrix between these transformations (α to β to ω).

The transformation mechanisms imply specific orientational relationships between transformed regions. Silcock¹³ suggested orientational relationships (OR II) with $(0001)_\alpha // (1120)_\omega$ and $[1120]_\alpha // [0001]_\omega$,⁹ which appears to be at odds with the *ab initio* calculations of electronic structures by Trinkle *et al.*⁷ who shows (OR I) with $(0001)_\alpha // (01\bar{1}1)_\omega$ and $[1120]_\alpha // [\bar{1}011]_\omega$. The pathway is named TAO-1 within the context of his paper^{7,8,14,15} and complies with nucleation models. A third pathway was proposed by Usikov and Zilbershtein (UZ pathway),¹⁶ in which the hcp- ω transformation

^{a)}Present address: State Key Laboratory of Tribology, Tsinghua University, Beijing 100084, China.

^{b)}Authors to whom correspondence should be addressed. Electronic addresses: dingxd@mail.xjtu.edu.cn and ekhard@esc.cam.ac.uk

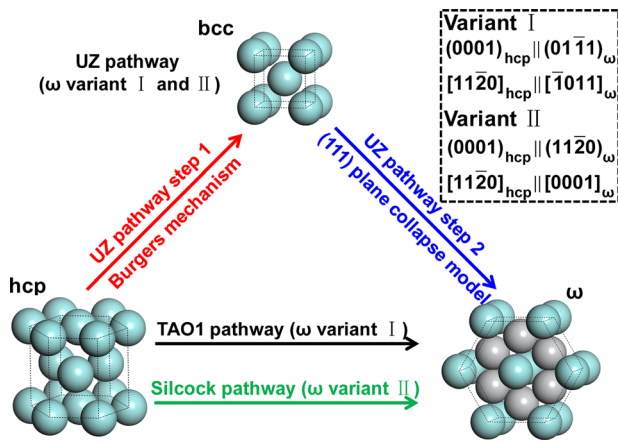


FIG. 1. Summary of proposed transformation mechanisms for the hcp- ω phase transformation and their corresponding ω variant product with respect to initial hcp phase, OR I with $(0001)_x \parallel (01\bar{1}1)_\omega$ and $[11\bar{2}0]_x \parallel [\bar{1}011]_\omega$ and OR II with $(0001)_x \parallel (11\bar{2}0)_\omega$ and $[11\bar{2}0]_x \parallel [0001]_\omega$.

proceeds via a transient bcc phase. As there are two equivalent $\{111\}_\beta$ plane collapse modes from bcc to ω phase,¹⁷ two types of ORs (OR I and OR II) between the initial hcp phase and the ω phase are possible. The UZ pathway consists of two steps: the hcp \rightarrow bcc transformation (Burgers mechanism)³⁰ and the bcc \rightarrow ω transformation ((111) plane collapse model).^{31,32} A summary of the possible pathways is shown in Fig. 1.

We use density functional theory (DFT) calculations to analyze the pathways of the homogeneous hcp- ω transformation in Zr and compare the results with new calculations for Ti. The enthalpy barriers were calculated using a generalized solid-state nudged elastic band (G-SSNEB) method,³³ all calculations were performed using the Vienna *ab-initio* simulation package (VASP).³⁴ The G-SSNEB method involves both atomic and unit-cell degrees of freedom and is designed to determine reaction pathways of solid-solid transformations. We used 12 atom supercells of the hcp, ω , and bcc

phases according to TAO1,⁷ UZ,¹⁶ and Silcock¹³ pathways (see supplementary material Fig. S1).³⁵ The lattice constants of the three phases under pressures are listed in Table S1.³⁵ Electron exchange and correlations were modeled within the generalized gradient approximation (GGA) using Perdew-Burke-Ernzerhof (PBE) form.³⁶ The plane wave basis kinetic energy cut off was set to 500 eV. The NEB calculation was considered to be complete when the total force of an atomic configuration was less than 0.01 eV/Å. For more calculation details see supplementary material.³⁵ We define the activation enthalpy as the enthalpy difference between the transition state and hcp phase ($\Delta H = H_{\text{transition}} - H_{\text{hcp}}$). Fig. 2 shows the activation enthalpies along the three transformation pathways for Ti and Zr, respectively.

The most simple pathway occurs in Ti. It does not change much with pressure (Figs. 2(a)–2(c)). The UZ pathway has the highest activation enthalpy at 0 GPa (Fig. 2(a)), the activation enthalpy for the Silcock pathway is intermediate and the TAO1 pathway has the lowest activation enthalpy. This sequence of activation enthalpies ($E_{\text{UZ}} > E_{\text{Silcock}} > E_{\text{TAO1}}$) does not change (Figs. 2(b) and 2(c)) with pressure up to 23 GPa. This result confirms that TAO1 is the correct pathway for the hcp- ω transformation in Ti under pressure.⁷

In contrast to Ti, the transition pathway of the hcp- ω transformation in Zr changes dramatically with pressure (Figs. 2(d)–2(f)). At zero pressure, the activation enthalpy is similar to that of Ti (Fig. 2(d)), with $E_{\text{UZ}} > E_{\text{Silcock}} > E_{\text{TAO1}}$ and does not change much in the low pressure regime (< 10 GPa, Fig. 2(e)). The activation enthalpy for the UZ pathway then decreases strongly with increasing pressure and becomes lowest at 23 GPa, and completely overlaps with the TAO1 pathway (Fig. 2(f)). The crystal structure of the metastable phases at 23 GPa, as shown in the insets of Fig. 2(f), are C2/c and bcc phase. In order to further identify the metastable bcc phase, we calculate the electron density of states (DOS) for hcp, ω , bcc, and the transient state (bcc) at 23 GPa (Fig. 3). The DOS of the bcc phase and transient state

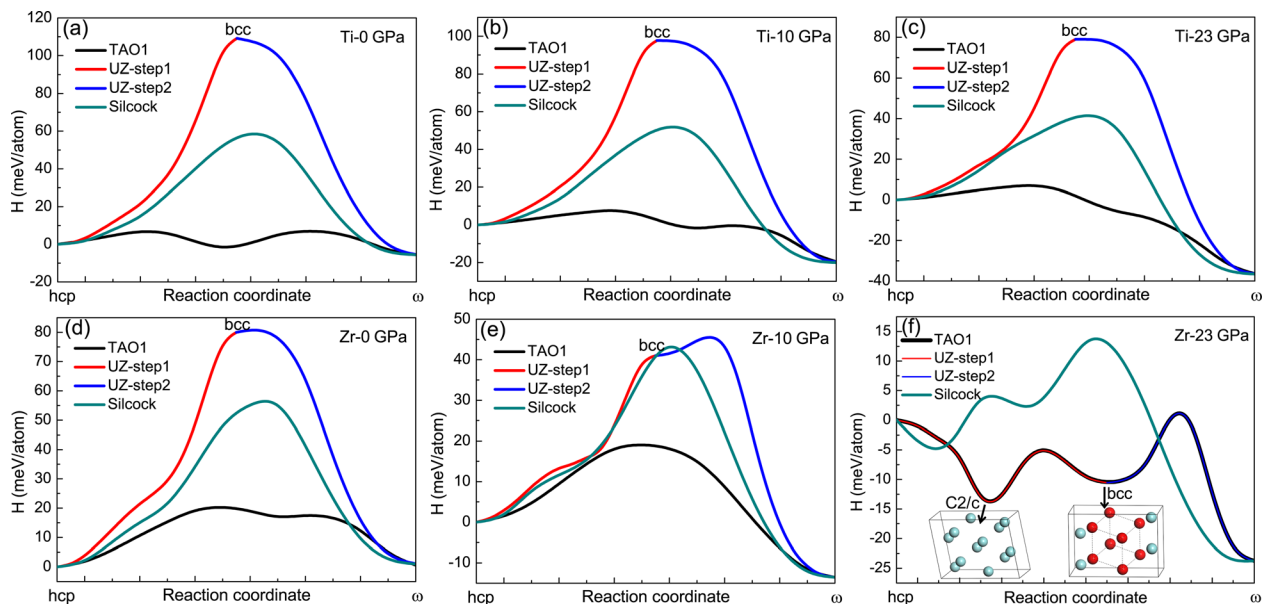


FIG. 2. The enthalpy landscape along three types of hcp- ω phase transformation pathways (TAO1 pathway, UZ pathway and Silcock pathway) of Ti and Zr. (a)–(c) The enthalpies along three pathways of Ti at 0 GPa, 10 GPa, and 23 GPa; (d)–(f) The enthalpies along the three pathways of Zr at 0 GPa, 10 GPa, and 23 GPa; insets in (f) represent the metastable phases along the hcp- ω phase transformation pathway.

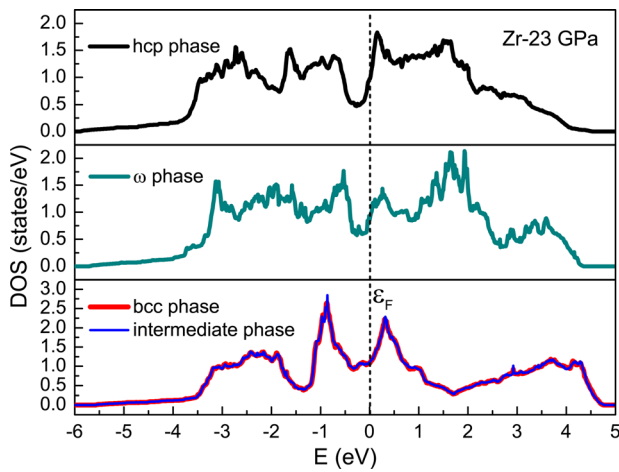


FIG. 3. Density of state (DOS) for hcp, ω , bcc, and transient phases in TAO1 pathway of Zr under 23 GPa.

are nearly identical (Fig. 3) and, in turn, very different from hcp and ω . This agreement confirms the transient phase at 23 GPa as bcc with the hcp- ω transformation following the UZ pathway.

A switch between transformation pathways occurs between 10 GPa and 19 GPa (Fig. 4). Starting from the hcp phase, we find that at 10 GPa the first change of the structural state under pressure is to activate the shuffle along $\langle 11\bar{2}3 \rangle$ directions. This is the dominant mechanism at low pressure. The transformation pathway at 19 GPa shows a very different picture: the shuffle along $\langle 11\bar{2}3 \rangle$ directions is suppressed and replaced by a combination of shear along $\langle 11\bar{2}0 \rangle$ directions and shuffle along $\langle 1\bar{1}00 \rangle$ directions. We relate this effect to the large c/a ratio in the hcp phase of Zr (Fig. 5). The larger

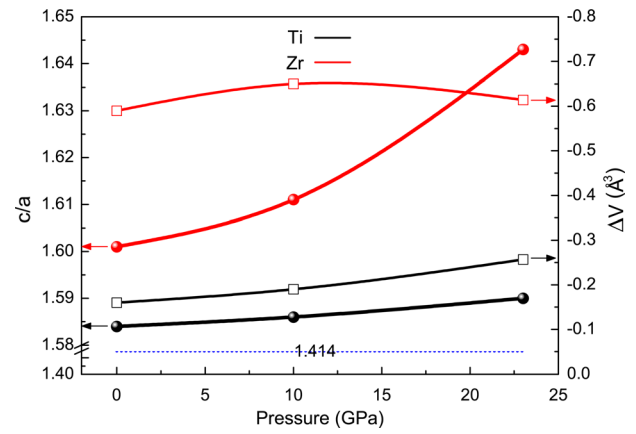


FIG. 5. Change of c/a ratio and volume for hcp-bcc phase transformation in Ti and Zr, which shows that the changes in Zr are dramatically larger than those of Ti.

c/a ratio has a strong effect on atomic cooperative movements during the hcp- ω transformation. The large c -axis eases the shuffle movement along the $\langle 1\bar{1}00 \rangle$ directions, while the relative decrease of the a -axis impedes the shuffle along $\langle 11\bar{2}3 \rangle$ or $\langle 11\bar{2}0 \rangle$ directions. As a result, the increase of the c/a ratio with pressure in Zr hinders the shuffle along the $\langle 11\bar{2}3 \rangle$ directions in Zr (Fig. 4).

The effect of pressure on the transformation pathways can be understood from a fundamental perspective if the order parameters for the hcp- ω transformation are considered (Fig. 4). The hcp- ω transformation includes three types of atomic cooperative movements in the hcp phase: the shuffle along the $\langle 1\bar{1}00 \rangle$ directions, the shear along the $\langle 11\bar{2}0 \rangle$ directions and the shuffle along the $\langle 11\bar{2}3 \rangle$ or $\langle 11\bar{2}0 \rangle$ directions (corresponding to two types of ORs). The first and

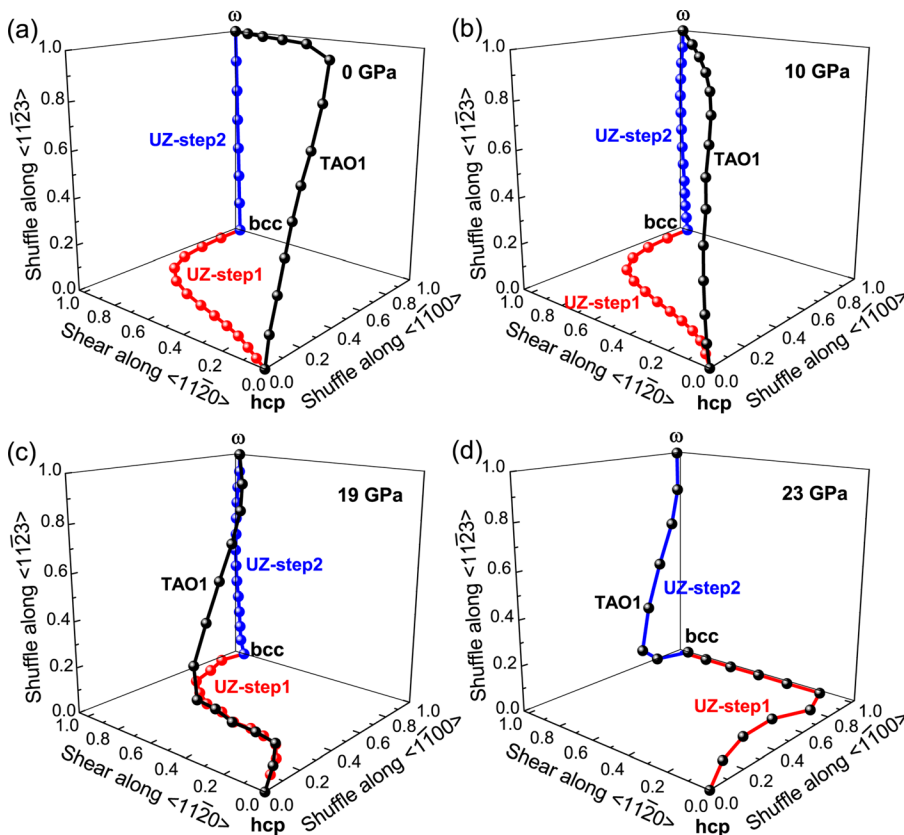


FIG. 4. Change of three types of atomic cooperative movements (the shuffle along the $\langle 1\bar{1}00 \rangle$ directions, the shear along the $\langle 11\bar{2}0 \rangle$ directions and the shuffle along the $\langle 11\bar{2}3 \rangle$ direction) in hcp- ω transformation of Zr under pressure of 0 GPa, 10 GPa, 19 GPa, and 23 GPa, respectively. Indicating the pressure induces the occurrence of bcc like transient state.

second atomic movements transfer hcp to bcc, while the third atomic movement in bcc $\langle 111 \rangle$ directions corresponds to the collapse during the bcc- ω transformation. The evolution of the order parameters with pressure changes very little in Ti (Figs. 2(a)–2(c)). In contrast, when the pressure in Zr increases to 10 GPa, the TAO1 pathway approaches the UZ pathway (Figs. 4(a) and 4(b)). The difference between the pathways decreases further with increasing pressure and leads to partial overlap (Fig. 4(c)). At 23 GPa (Fig. 4(d)), the TAO1 pathway completely overlaps with the UZ pathway. The main pressure dependence can now be identified as the shuffle along the $\langle 11\bar{2}3 \rangle$ directions. This shuffle is an inherent part of the TAO1 pathway at low pressure while it is eliminated from the first part of the high pressure pathway (UZ step 1 in Fig. 4(d)). The lack of the $\langle 11\bar{2}3 \rangle$ directions shuffles at the beginning of the transformation that stabilizes the bcc transient phase at high pressure.

Thermodynamic analyses in the supplementary material³⁵ demonstrate that the driving force for the occurrence of hcp-bcc transformation in Zr under high pressure arises from the $P\Delta V$ term. The large c/a ratio contributes to the excess volume of the hcp phase compared with the bcc phase (Fig. 5). According to the Burgers mechanism, the hcp cell transfers to the bcc cell during the transformation. From the lattice constants of the two phases in Ti and Zr, we find that the areas of the basal planes in the two cells are nearly the same. The volume change arises from the shrinkage of c axis ($[0001]$ direction) in the hcp cell. The shrinkage of c axis in the hcp-bcc phase transformation is mirrored by the c/a ratio, which converges to $\sqrt{2}$ during the transformation. The large change of the c/a ratio in Zr corresponds to the change of the electronic structure of Zr with weaker interactions along $[0001]$ direction and stronger interactions along $[1120]$ direction (in comparison with Ti, see supplementary material Fig. S2).³⁵ We expect changes of the c/a ratio under pressure and a sudden change of transformation pathways because the shuffle along the $\langle 11\bar{2}3 \rangle$ directions is impeded at high pressure at the early stage of the transformation pathway.

In addition, the metastability of the high pressure transformation in Zr (Fig. 2(f)) is clearly seen by the decrease of the activation barrier with increasing pressure. While low pressure transformations are thermally inhibited by an activation energy, we find that the high pressure pathway shows a straight energy decrease to the first metastable phase and then rather low activation energies (less than 11.56 meV) for the second metastable bcc phase and the final ω phase. Each hump is smaller than the one big hump at low pressure in Fig. 2(d) (ca. 20.24 meV).

The transient bcc phase has not been seen in equilibrium experiments. According to our results, we would expect this effect at much higher pressure than previously expected. Experimental works on Zr or Zr-2.5%Nb alloy by Perez-Prado *et al.*^{5,37} does see the β phase at lower pressure and it may well be that this observation is supported by the non-uniform (shear) stress applied to the sample.³⁸ More detailed works on pathway under shear stress and experiments at high hydrostatic pressure are needed to further clarify the phase metastability.

We are grateful to NSFC (51320105014, 51321003) for their support. EKHS is grateful to EPSRC (EP/K009702/1) and the Leverhulme Trust (EM-2016-004).

- ¹Q. Yu, L. Qi, T. Tsuru, R. Traylor, D. Rugg, J. W. Morris, Jr., M. Asta, D. C. Chrzan, and A. M. Minor, *Science* **347**, 635 (2015).
- ²E. Clouet, D. Caillard, N. Chaari, F. Onimus, and D. Rodney, *Nat. Mater.* **14**, 931–936 (2015).
- ³D. Banerjee and J. C. Williams, *Acta Mater.* **61**, 844 (2013).
- ⁴H.-R. Wenk, P. Kaercher, W. Kanitpanyacharoen, E. Zepeda-Alarcon, and Y. Wang, *Phys. Rev. Lett.* **111**, 195701 (2013).
- ⁵M. T. Perez-Prado and A. P. Zhilyaev, *Phys. Rev. Lett.* **102**, 175504 (2009).
- ⁶R. Ahuja, L. Dubrovinsky, N. Dubrovinskaia, J. M. O. Guillen, M. Mattesini, B. Johansson, and T. L. Bihan, *Phys. Rev. B* **69**, 184102 (2004).
- ⁷D. R. Trinkle, R. G. Hennig, S. G. Srinivasan, D. M. Hatch, M. D. Jones, H. T. Stokes, R. C. Albers, and J. W. Wilkins, *Phys. Rev. Lett.* **91**, 025701 (2003).
- ⁸R. G. Hennig, D. R. Trinkle, J. Bouchet, S. G. Srinivasan, R. C. Albers, and J. W. Wilkins, *Nat. Mater.* **4**, 129–133 (2005).
- ⁹S. K. Sikka, Y. K. Vohra, and R. Chidambaram, *Prog. Mater. Sci.* **27**, 245 (1982).
- ¹⁰X. Yu, R. Zhang, D. Weldon, S. C. Vogel, J. Zhang, D. W. Brown, Y. Wang, H. M. Reiche, S. Wang, S. Du, C. Jin, and Y. Zhao, *Sci. Rep.* **5**, 12552 (2015).
- ¹¹Y. Zhao and J. Zhang, *Appl. Phys. Lett.* **91**, 201907 (2007).
- ¹²D. W. Brown, J. D. Almer, L. Balogh, E. K. Cerreta, B. Clausen, J. P. Escobedo-Diaz, T. A. Sisneros, P. L. Mosbrucker, E. F. Tulk, and S. C. Vogel, *Acta Mater.* **67**, 383 (2014).
- ¹³J. M. Silcock, *Acta Metall.* **6**, 481 (1958).
- ¹⁴D. R. Trinkle, M. D. Jones, R. G. Hennig, S. P. Rudin, R. C. Albers, and J. W. Wilkins, *Phys. Rev. B* **73**, 094123 (2006).
- ¹⁵D. R. Trinkle, D. M. Hatch, H. T. Stokes, R. G. Hennig, and R. C. Albers, *Phys. Rev. B* **72**, 014105 (2005).
- ¹⁶M. P. Usikov and V. A. Zilbershtein, *Phys. Status Solidi A* **19**, 53 (1973).
- ¹⁷E. S. K. Menon, *Scr. Metall.* **16**, 717 (1982).
- ¹⁸D. Errandonea, Y. Meng, M. Somayazulu, and D. Hausermann, *Physica B* **355**, 116 (2005).
- ¹⁹E. Cerreta, G. T. Gray III, R. S. Hixson, P. A. Rigg, and D. W. Brown, *Acta Mater.* **53**, 1751 (2005).
- ²⁰S. Song and G. T. Gray III, *Philos. Mag. A* **71**, 275 (1995).
- ²¹G. Jyoti, K. D. Joshi, S. C. Gupta, and S. K. Sikka, *Philos. Mag. Lett.* **75**, 291 (1997).
- ²²P. S. Ghosh, A. Arya, R. Tewari, and G. K. Dey, *J. Alloys Compd.* **586**, 693–698 (2014).
- ²³S. C. Gupta, S. K. Sikka, and R. Chidambaram, *Scr. Metall.* **19**, 1167 (1985).
- ²⁴K. Shozugawa, N. Nogawa, and M. Matsuo, *Environ. Pollut.* **163**, 243–247 (2012).
- ²⁵L. Liu and W. A. Bassett, *Elements, Oxides, and Silicates: High-Pressure Phases with Implications for the Earth's Interior* (Oxford University Press, New York, 1986).
- ²⁶B. R. Hacker, W. C. McClelland, and J. G. Liou, “Ultrahigh-pressure metamorphism: Deep continental subduction,” *Geol. Soc. Am. Spec. Pap.* **403**, 206 (2006).
- ²⁷M. K. Jacobsen, N. Velisavljevic, and S. V. Sinogeikin, *J. Appl. Phys.* **118**, 025902 (2015).
- ²⁸H. Dammak, A. Dunlop, and D. Lesueur, *Nucl. Instrum. Methods Phys. Res., Sect. B* **107**, 204–211 (1996).
- ²⁹Y. K. Vohra, S. K. Sikka, E. S. K. Menon, and R. Krishnan, *Acta Metall.* **28**, 683–685 (1980).
- ³⁰L. Gao, X. Ding, H. Zong, T. Lookman, J. Sun, X. Ren, and A. Saxena, *Acta Mater.* **66**, 69 (2014).
- ³¹D. De Fontaine, *Acta Metall.* **18**, 275 (1970).
- ³²B. A. Hatt and J. A. Roberts, *Acta Metall.* **8**, 575 (1960).
- ³³D. Sheppard, P. Xiao, W. Chemelewski, D. D. Johnson, and G. Henkelman, *J. Chem. Phys.* **136**, 074103 (2012).
- ³⁴G. Kresse and J. Furthmüller, *Phys. Rev. B* **54**, 11169 (1996).
- ³⁵See supplementary material at <http://dx.doi.org/10.1063/1.4959864> for the G-SSNEB calculation details in Ti and Zr under hydrostatic pressures and electronic understanding of the c/a ratio difference between Ti and Zr.
- ³⁶J. P. Perdew, K. Burke, and M. Ernzerhof, *Phys. Rev. Lett.* **77**, 3865 (1996).
- ³⁷A. P. Zhilyaev, A. V. Sharafutdinov, and M. T. Perez-Prado, *Adv. Eng. Mater.* **12**, 754 (2010).
- ³⁸H. Zong, T. Lookman, X. Ding, C. Nisoli, D. Brown, S. R. Niezgoda, and J. Sun, *Acta Mater.* **77**, 191 (2014).